Link sito dell'editore: https://ieeexplore.ieee.org/xpl/RecentIssue.jsp?punumber=22

Link codice DOI: https://ieeexplore.ieee.org/document/7286873

Citazione bibliografica dell'articolo:

G. Monti, P. Arcuti and L. Tarricone, "Resonant Inductive Link for Remote Powering of Pacemakers," in *IEEE Transactions on Microwave Theory and Techniques*, vol. 63, no. 11, pp. 3814-3822, Nov. 2015, doi: 10.1109/TMTT.2015.2481387.

Resonant Inductive Link for Remote Powering of Pacemakers

G. Monti, P. Arcuti, and L. Tarricone

***Abstract*—This paper presents a wireless power link for powering implantable medical devices. The proposed link operates at 403 MHz and exploits magnetic coupling between an external resonator and an implanted resonator to wirelessly provide power to implantable devices. Experimental results for remote powering of pacemakers are reported and the compliance with safety guidelines is discussed. It is demonstrated that the proposed wireless link is able to deliver up to 1 mW with an induced 10-g average Specific Absorption Rate lower than 1.08 W/kg. This value is significantly below the 2 W/kg recommended limit, thus proving the suitability of the proposed system to be used to energize modern pacemakers.**

***Index Terms*— Implantable medical device, pacemaker, RF-to-DC conversion, resonant inductive link, specific absorption rate (SAR), wireless power transfer.**

I. Introduction

Nowadays, medical implantable devices are increasingly used for the treatment of important diseases, such as cardiac pathologies or acute forms of diabetes. In order to improve the performance of these devices, a key role is played by wireless technologies for data and power transmission.

In fact, wireless communication between medical implants and an external controller is commonly adopted to collect important bio-information which is essential for diagnostic and therapeutic applications.

Data links for medical devices that have been proposed up to now in the literature, are mainly based on the use of compact printed implantable antennas [1]-[4]. The choice of the operating frequency is dictated by the rules of the RF spectrum management which reserve the MedRadio (Medical Device Radiocommunications) service band [5] for Medical Implant Communications Service (MICS) devices.

As for issues related to power, in many implantable devices the energy necessary to operate is provided by a small lithium ion battery embedded in the device. Although the lithium ion technology represents a good choice to obtain compact dimensions, high efficiency and extended lifetime, the battery still occupies almost half of the total volume of the medical device and its life time varies from few years to tens of years. Furthermore, replacing the battery requires surgery, which implies discomforts and risks to the patient health.

G. Monti, P. Arcuti, and L. Tarricone are with the Department of Engineering for Innovation, University of Salento, Via per Monteroni, Lecce 73100, Italy (email: {giuseppina.monti, paola.arcuti, luciano.tarricone}@unisalento.it).

In this regard, the use of a wireless power transfer (WPT) approach [6]-[16], combined with high performance energy storage devices (such as supercapacitors) would represent an attractive solution to lengthen the life time of common medical implants.

The most widely adopted method to implement WPT relies on a capacitive or inductive coupling between a transmitter connected to a power source and a receiver connected to the device to be powered.

Despite the advantages related to the use of a WPT solution for powering electronic devices, in the case of implantable medical devices, there are some practical problems that complicate its applicability. In fact, when a wireless link for data or power transmission has to be established with a medical implant, the receiver has to work inside the human body under one or more layers of human tissue which represent a hostile environment for wave propagation being characterized by very high values of loss.

A figure of merit that can be used to evaluate the performance of the wireless link is the *power transfer efficiency* (η) expressed by:

$$\eta\ (\%) = \frac{P_{RIC}}{P_{AC}} \text{ x } 100 \qquad (1)$$

being P_{AC} the power delivered to the transmitter, while P_{RIC} is the power delivered by the receiver to the implanted device.

It is worth underlining that requirements for η for data and power links are very different. In the case of a wireless data link, very low values of η are sufficient for a proper data transmission. Conversely, in the case of a WPT link η is the most important figure of merit: values that allow providing the medical device with the power it needs to operate are needed.

In this regard, the use of resonant inductive coupling seems to be the best solution to maximize the link efficiency. Indeed, the use of a transmitter and a receiver resonating at the same frequency combined with magnetic coupling maximizes the power transfer efficiency (η) while minimizing the interaction with the surrounding environment.

In order to minimize losses due to human tissues, most of the WPT systems presented until now in the literature operate at low frequencies. The typical working frequency is from few kHz to tens of MHz [9]-[12]. This choice is related to considerations on electromagnetic energy absorption in human tissues which increases with frequency.

In particular, in [9] a system working at 100 kHz and consisting of two spiral inductors is proposed. Results of in vivo tests are reported demonstrating η up to 16% at a

distance of 8 mm.

Devices working in the MHz range are proposed in [10]-[12]. In [10], the energy link is implemented by means of two printed spiral coils resonating at 13.56 MHz. Experimental tests performed by using a slice of beef to simulate the presence of human tissues are reported. In the case of a link optimized to work in a muscle environment a value of η of about 30% is demonstrated at a distance of 10 mm.

Similarly, the system proposed in [11] works at 13.56 MHz and uses two resonant spiral coils. Very high values of the energy transfer efficiency are obtained thanks to the use of a circuit for resonant load transformation. From tests performed using a layer of pork, values of η of about 58% are obtained at a distance of 10 mm.

Finally, in [12] a system consisting of two resonant coils for wireless energy transfer and integrating an antenna for biotelemetry applications is proposed. The WPT link works at 6.78 MHz and, from tests performed in air, has a transfer efficiency of about 38%. As for the antenna, it works in the MICS band and a test in vitro demonstrated a gain of about -27 dBi.

In [13], with reference to mm-sized receiving antennas/coils, theoretical and numerical studies are reported demonstrating the convenience of operating in the GHz range. According to these results, in [14] a wirelessly powered miniature implant for optogenetic stimulation is presented. The WPT link is implemented at 1.6 GHz with a receiver of dimensions (3x3) mm^2. From tests performed with a block of porcine tissue, at a distance of 1 cm the received power is about 300 μW when the output power of the transmitter is 500 mW, thus corresponding to a transfer efficiency lower than 0.06%.

As evidenced from the above, the choice that is usually adopted in the literature is to operate in the MedRadio band (or other bands reserved for medical devices) for data transmission, while frequencies not reserved for medical applications (typically up to ten of MHz) ae used for power transfer. This choice has two important drawbacks: 1) the need of using two separate devices for data and power transmission, 2) possible interference problems for the link implementing the power transfer.

With regard to point 2), frequencies from some kHz up to some MHz are commonly adopted for implementing high power WPT links for general purpose applications (i.e., powering of electric vehicles and common electronic devices). Furthermore, the 13.56 MHz frequency adopted in [7]-[8] is used for Near Field Communication systems. As for systems operating in the GHz range [11]-[12], they could have interference problems with wireless communication systems. In addition, it should be noticed that WPT systems proposed in [11]-[12] are characterized by very low values of η, so that they are well suited for devices with a very low power consumption and for which the crucial aspect is the size of the receiver to be implanted.

A promising solution to overcome the aforementioned problems, could be the use of systems operating in the MedRadio service band [14]. In fact, the use of a band reserved for medical devices would minimize interference problems. Furthermore, the same device used for powering the implanted medical device could be used for remote monitoring purposes. As for aspects related to tissue absorption, a working frequency in the order of some hundreds of MHz, is a solution worth to be investigated. In fact, it could represent a good comprise in order to obtain receivers with compact dimensions and acceptable values of η.

Accordingly, a system operating at 434 MHz (i.e., in the ISM-industrial, scientific and medical band) was experimentally investigated by the authors in [16]. In more details, in [16] we proposed a WPT system consisting of two segmented planar resonators. The dimensions of the receiver are (27x27) mm^2 and from measurements η has a value of about 4.6% at a distance of 15 mm.

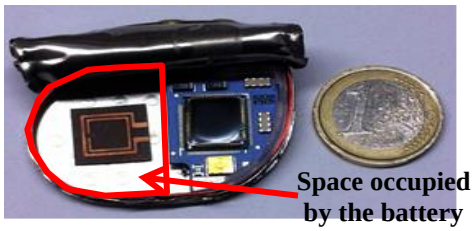

Fig. 1: Comparison between the proposed receiver and a single chamber non-rate responsive DISCOVERY II pacemaker (model 481) by Guidant.

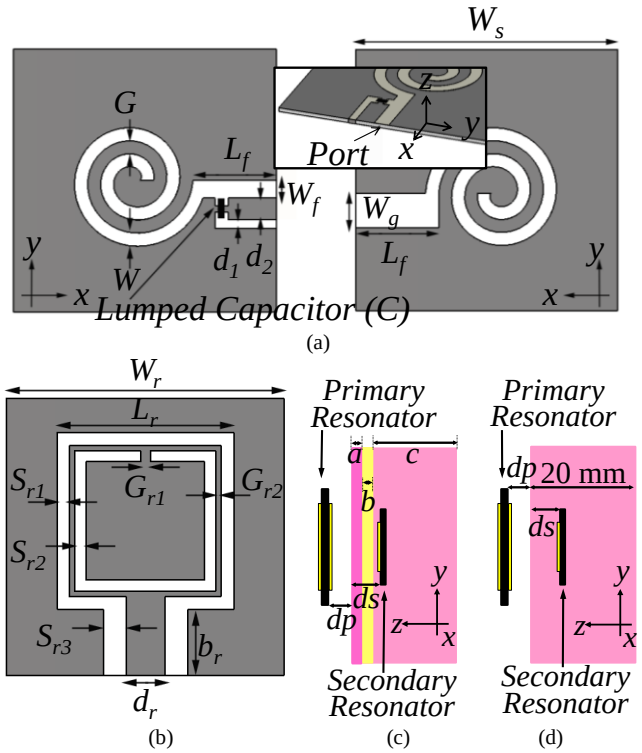

Fig. 2. Geometry of the primary resonator: (a) front and back view. (b) Geometry of the secondary resonator. Configurations adopted in full-wave simulations: (c) three-tissue layers model (skin-fat-muscle) with $dp = ds = 5$ mm, $a = b = 2$ mm and $c = 16$ mm (d) homogeneous model with $dp = ds = 5$ mm.

With respect to the solution proposed in [16], an improved WPT link for the powering of pacemakers is proposed in this

paper. In more detail, we propose a WPT system operating at 403 MHz which exactly falls in the MedRadio Service core band. The presented link uses two inductively coupled resonators, each one consisting of a compact loop. The receiver is a single face planar split ring resonator with dimensions of about (9.5x13.1) mm^2, thus resulting in a size reduction with respect to the solution proposed in [16] of about 89%. In this regard, it is worth underlining that the use of a planar solution for the receiver enables easy integration with common medical implants. Fig. 1 compares the proposed receiver with a single chamber non-rate responsive DISCOVERY II pacemaker (model 481) by Guidant. It can be seen that, with respect to the lithium battery, the proposed device occupies smaller space and, being planar, it could be easily placed on the front or back face of the electronic circuitry.

As for performance, it is shown that despite being the operating frequency characterized by high values of the absorption in human body, the proposed system exhibits good performance and is able to guarantee the energy requirements of modern pacemakers. From experimental tests performed by using minced pork to simulate the presence of human tissues, a power transfer efficiency of 5.24% is demonstrated at a distance of 1 cm.

These results suggest that the solution presented in this paper is an optimum alternative to WPT systems proposed up to now in order to minimize interference problems. Furthermore, it represents a promising solution for using the same device for powering and monitoring applications.

The paper is structured as follows. The proposed resonant inductive link is briefly described In Sect. II. Numerical and experimental data are given in Sect. III and discussed in Sect. IV. Finally, conclusions are drawn in Section IV.

TABLE I
ELECTRIC PARAMETERS ADOPTED IN FULL-WAVE SIMULATIONS FOR HUMAN TISSUES

403MHz	Skin	Fat	Muscle	One-Layer
ε_r	46.7	11.6	57.1	59.2
σ (S/m)	0.68	0.081	0.797	0.84

Note: Tissue properties have been taken by the IT'IS Foundation database [19].

II. PROPOSED RESONANT INDUCTIVE LINK

The proposed wireless power transmission system is based on magnetic coupling between two resonant planar loops: an external resonator (primary resonator) connected to a power source and an implanted resonator (secondary resonator) connected to the medical device (see Fig. 2). Both the transmitter and the receiver were designed on an Arlon 880 substrate (ε_r = 2.17, *tan(δ)* = 0.0009) with a thickness of 0.508 mm.

The primary resonator consists of two spirals printed on the top and bottom face of the Arlon substrate (see Fig. 2a), working as signal and ground trace. In order to tune the resonance frequency to the desired value, an SMD (Surface Mounted Device) capacitor in shunt configuration is also used.

As for the secondary resonator, a good magnetic coupling with the primary loop was obtained by using a square Split-Ring Resonator [17]. The dimensions of both the receiver and the transmitter were optimized by means of full-wave simulations performed by using the transient solver of CST Microwave Studio.

In more detail, the design process of the link was carried out as follows. We firstly designed the primary resonator by using a spiral geometry [18]. The parameters of the spiral were optimized by means of full-wave simulations so to have a compact area and a resonance frequency at 403 MHz. After that, we designed the secondary resonator. Firstly, we investigated the use of the same spiral geometry adopted for the primary resonator. Performance obtained in this way for the link was not satisfactory. In fact, the maximum value obtained for the transmission coefficient was about -20 dB. Then, taking into account the extensive literature on SRRs demonstrating their strong magnetic response, we investigated the use of a square SRR for the secondary resonator (see Fig. 2b). A preliminary analysis of a link using a spiral inductor for the primary resonator and an SRR for the secondary resonator demonstrated that this configuration was able to guarantee good magnetic coupling.

According to these results, the design process was carried out with full-wave optimizations of the overall link taking into account the presence of biological tissues.

With reference to the application of the proposed wireless link for powering a pacemaker, we assumed that the receiver will be implanted at a depth of 5 mm in a layer of muscle, below a 2 mm layer of skin and a 2 mm layer of fat (see Fig. 2c). The electromagnetic parameters adopted for human tissues are given in Table I.

The presence of a biocompatible coating on the surfaces of the secondary resonator was taken into account in simulations. In particular, we assumed a coating layer of parylene C with a dielectric constant of 2.9 and a thickness of 1 μm. The final dimensions of the two resonators are summarized in Table II. Fig. 3 shows the scattering parameters calculated by means of full-wave simulations when the resonators are placed at a distance (*dp*) of 5 mm.

In view of experimental tests reported in the next section and based on the use of minced pork, scattering parameters corresponding to full-wave simulations performed by approximating the three layers of tissue (skin-fat-muscle) with a homomogeneous effective medium (see Fig. 2d) were also calculated. In more detail, we determined the electromagnetic parameters of a homogeneous medium resulting in a good approximation of the three-layer model illustrated in Fig. 2c.

From full-wave simulations, a good matching between data corresponding to the two models was obtained by assuming the following parameters for the effective homogeneous medium: ε_r = 59.2 and σ = 0.84 S/m. A comparison between results corresponding to the use of the homogeneous effective medium (see Fig. 2d) and the ones corresponding to the use of the three-tissue layers (see Fig. 2c) is given in Fig. 3.

A good agreement for the scattering parameters corresponding to the two models can be noticed, thus

confirming that the homogeneous medium is a reliable approximation. From full-wave simulations illustrated in Fig. 3 it can be seen that the working frequency of the resonant link is in the MedRadio band. In more details, in the case of the homogeneous model the link exhibits a transmission coefficient with a maximum of -11.2 dB at 403 MHz. While, in the case of the three tissue layers the link exhibits a transmission coefficient with a maximum of -9.55 dB at 406 MHz. Consistently with this homogeneous model, in the next section results of experimental tests perfomed by using minced pork are reported and discussed.

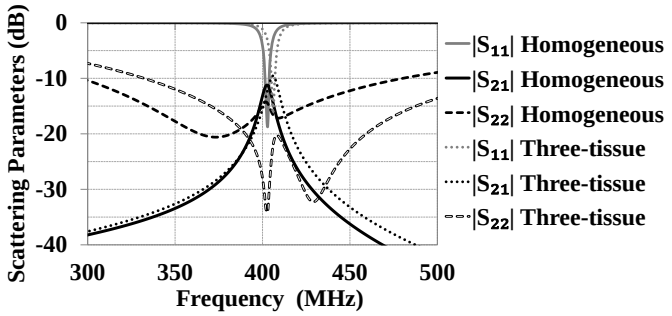

Fig. 3. Scattering parameters calculated by means of full-wave simulations for the configuration illustrated in Fig. 2c and the one of Fig. 2d when dp = ds = 5 mm.

(a) (b)

Fig. 4. Photographs of the two prototypes realized on Arlon 880 substrate: (a) front and back view of the primary resonator, (b) secondary resonator.

Fig. 5. Experimental setup adopted to verify the performance of the proposed resonant inductive link. The photograph shows the primary resonator at a distance dp = 5 mm from minced pork, while the secondary resonator is inside minced pork at a depth ds = 5 mm.

TABLE II
DIMENSIONS OF THE RESONATORS ILLUSTRATED IN FIG. 2

Primary Resonator		Secondary Resonator	
Symbol	Value	Symbol	Value
W_s	30 mm	W_r	14.9 mm
G	1.5 mm	L_r	9.5 mm
W	1.5 mm	G_{r1}	0.53 mm
L_f	9.5 mm	G_{r2}	0.28 mm
W_f	2 mm	S_{r1}	0.69 mm
d_1	1 mm	S_{r2}	0.59 mm
d_2	2.5 mm	S_{r3}	1.22 mm
W_g	4 mm	b_r	3.56 mm
C	27 pF	d_r	2.07 mm

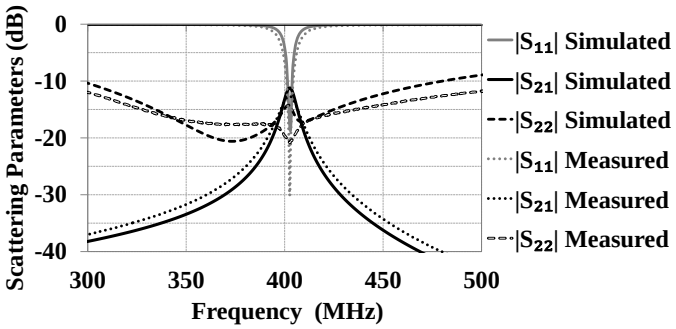

Fig. 6. Scattering parameters of the proposed inductive link: comparison between simulation results and experimental data.

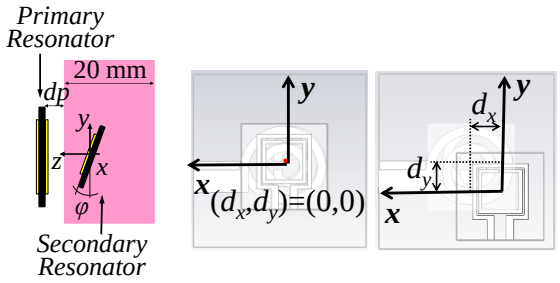

(a) (b)

Fig. 7. Configuration adopted in order to evaluate the performance of the proposed WPT link in the case of a misalignment between the transmitter and the receiver. (a) Rotation of the secondary resonator around the x-axis. (b) Displacement along the x- and y-axis with respect to the optimum position (i.e., d_x = d_y = 0).

TABLE III
COMPARISON OF THE PROPOSED WPT LINK WITH THOSE PROPOSED IN [9]-[12] AND [14]

Ref.	Operating Frequency	Geometry of the receiver	Dimensions (mm^2)	Efficiency/Gain
[9]	100 kHz	Spiral coil	(8x8)	16% @ 8 mm
[10]	13.56 MHz	Spiral coil	(10x10)	30%@1 cm
[11]	13.56 MHz	Resonant Spiral coil	(25x10)	58%@1 cm
[12]-WPT link	6.78 MHz	Resonant Spiral coil	(12x12)	38% @ 2 cm in air
[12]-Data link	MICS band [402-405] MHz	loop loaded with a magnetic core	(12x12)	-27dBi
[14]	1.6 GHz	multi-turn coil	(3x3)	0.06% @ 1 cm
This work	MedRadio band [401-406] MHz	Resonant Square Split ring resonator	(9.5x9.5)	5.24% @ 1 cm

III. EXPERIMENTAL AND NUMERICAL RESULTS

A prototype of both the primary and the secondary resonator was fabricated on an Arlon 880 substrate (see Fig. 4).

In order to verify the performance of the proposed inductive link in the presence of human tissues we used minced pork [20]-[21]. In fact, it was experimentally verified that in the frequency range of interest pork loin has electromagnetic

parameters very close to the homogeneous effective medium described in the previous section. The setup adopted for measurements is illustrated in Fig. 5.

According to the configuration illustrated in Fig. 2d, tests were performed by placing the secondary resonator inside minced pork at a depth ds = 5 mm, while the primary was placed outside at a distance dp = 5 mm.

The R&S® ZVL6 vector network analyzer was used to measure the scattering parameters of the proposed link. Corresponding results are given in Fig. 6 and compared with numerical data of the homogeneous medium model. It can be seen that excellent agreement was obtained. From measurements the frequency of resonance is 403 MHz and at this frequency the scattering parameters are: $|S_{11}|$ = -30 dB, $|S_{22}|$ = -20.8 dB and $|S_{21}|$ = -12.7 dB.

The power transfer efficiency of the proposed inductive link can be evaluated by using the scattering parameters to calculate the power delivered to the implanted device:

$$P_{RIC} = P_{AC}|S_{21}|^2(1-|S_{11}|^2)(1-|S_{22}|^2) \quad (2)$$

According to (1)-(2), at 403 MHz η is 5.24% from experimental data and 7.3% from numerical data.

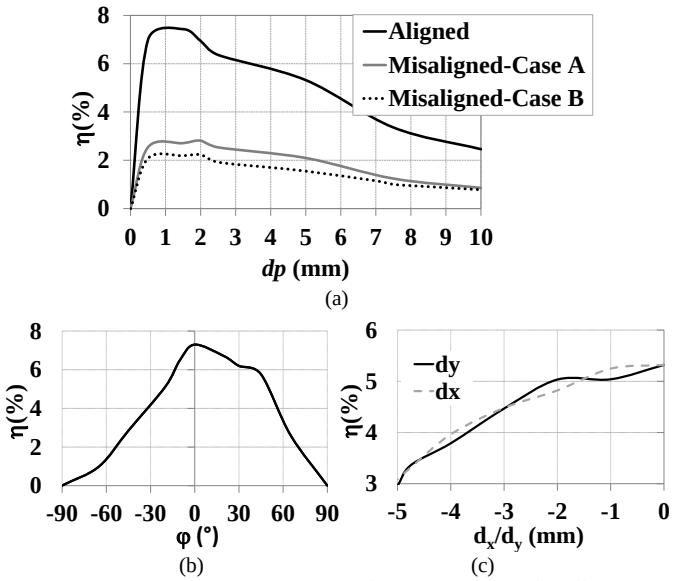

Fig. 8. (a) Experimental data obtained for the power transfer efficiency in the case of misalignment between the two resonators: Case A corresponds to the primary resonator parallel to the *xy*-plane and the secondary resonator tilted by 45°, while Case B corresponds to both resonators parallel to the *xy*-plane and a displacement $d_x = d_y = L_r/2$. (b)-(c) Full-wave simulation results obtained for possible misalignment of the two resonators: (b) power transfer efficiency calculated for $dp = ds$ = 5 mm and by varying the rotation angle (φ) of the secondary resonator around the *x*-axis (the position φ = 0° corresponds to the secondary resonator parallel to the *xy*-plane), (c) power transfer efficiency calculated for $dp = ds$ = 5 mm and by varying the displacement d_x and d_y along the *x*- and *y*–axis.

A comparison of the proposed link with those proposed in [9]-[12] and [14] is provided in Table III: it can be seen that the solutions proposed in [9]-[12] for the WPT link share a planar solution to facilitate integration. It can be also noticed that the proposed receiver has dimensions comparable (in most cases smaller) with that proposed in the literature. As for efficiency, in the following part of this section it will be demonstrated that the value of 5.24% is enough to provide up to 1 mW while inducing a 10-g average SAR lower than 1.08 W/kg. This result proves that the proposed link is able to provide modern pacemakers with the power they need in compliance with safety regulations.

A. Sensitivity Analysis

The sensitivity of the performance of the proposed WPT link to the distance and to misalignment between the two resonators was also evaluated.

Fig. 7 illustrates the configurations adopted for the case of a misalignment between the two resonators. With respect to the position of optimum alignment and referring to Fig. 7, we considered the cases of: 1) a rotation of the secondary resonator around the *x*-axis (the optimum position is the one corresponding to both resonators parallel to the *xy*-plane, see Fig. 7a), 2) a displacement d_x along the *x*-axis (see Fig. 7b), 3) a displacement d_y along the *y*-axis (see Fig. 7b). Measurements were performed for:

- case A corresponding to the primary resonator parallel to the *xy*-plane and the receiver tilted by 45° (see Fig. 7a),

-case B corresponding to a displacement $d_x = d_y = L_r/2 \cong 5$ mm, being L_r the dimension of the external square ring of the secondary resonator (see Fig. 2b and Fig. 7b).

Results obtained in this way for different values of dp (i.e., the distance of the transmitter from the minced pork) are given in Fig. 8a. In the case of aligned resonators, a maximum of the transfer efficiency of about 7.4% was obtained for dp equal to 1.5 mm.

As for the case of misalignment, from Fig. 8a it can be noticed that performance degrades significantly. In more detail, in the case of a 45° rotation around the *x*-axis, the conversion efficiency is lowered by 3-5% percentage points for a value of dp in the range of [0.5, 4] mm.

In particular, the maximum value obtained for η is of about 2.8% and has been obtained for dp = 2 mm. Similar results were obtained for the case of a displacement $L_r/2$ along the *x*- and *y*-axis. The maximum value of η has been measured for dp = 1.5 mm and is of about 2.4%.

Further investigations were performed by means of full-wave simulations. Corresponding results are summarized in Figs. 8 (b)-(c). It can be seen that in the case of a rotation around the *x*-axis of the secondary resonator, efficiency drops very quickly for values of the rotation angle (i.e., φ) greater than ±30°.

As for the case of displacement along the *x*- and *y*-axis, η reduces slowly and steadily increasing the displacement. As expected, according to the symmetry of the two resonators, a similar behavior was obtained for a displacement along the two axes.

B. AC/DC Conversion

Finally, in order to verify the suitability of the proposed WPT link to be used for the powering of a pacemaker,

experimental tests were performed by connecting to the secondary resonator an AC to DC converter (see Fig. 9a).

In more details, we designed a full bridge rectifier using the integrated HSMS-2828. A photograph and the equivalent circuit of the realized prototype is given in Fig. 9b. Taking into account that the input impedance of the receiver loop is 50 Ω and that the typical input impedance of a pacemaker is in the range of some hundreds of kΩ to some MΩ, the rectifier was optimized to be matched to 50 Ω at the input port and to 1 MΩ at the output port.

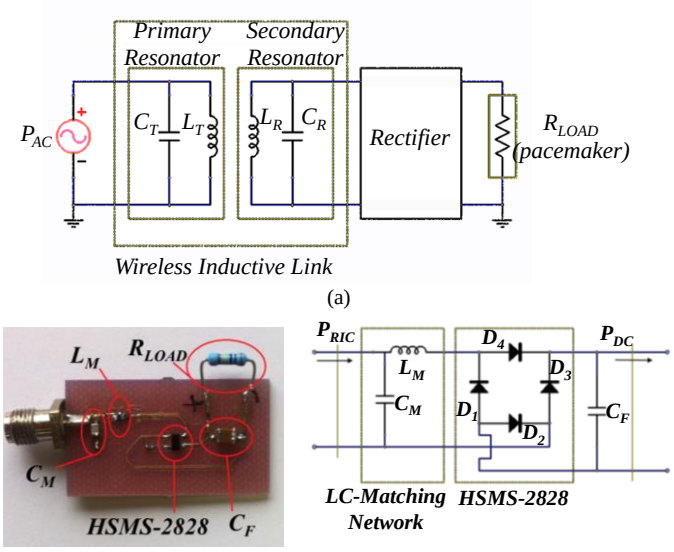

Fig. 9. (a) Schematic representation of the proposed WPT system. Photograph (b) and schematic representation (c) of the realized rectifier (L_M = 56 nH, C_M = 15 pF and C_F = 10 µF).

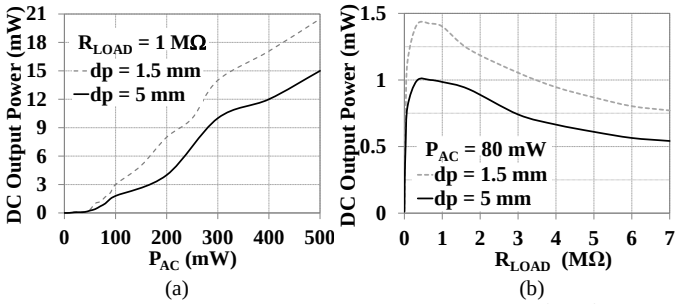

Fig. 10. Experimental results obtained by connecting the rectifier of Fig. 9 to the secondary resonator. (a) DC output power delivered to a load of 1 MΩ as function of the power provided to the primary resonator (P_{AC}). (b) DC output power as function of the load.

Tests were carried out by connecting the secondary resonator to the input port of the rectifier. As for the relative position of the two resonators, we considered the case of aligned resonators and two different values of the distance of the primary resonator from the minced pork (i.e., *dp*). In more detail, experimental data were taken for *dp* = 1.5 mm, that is the value of *dp* corresponding to the maximum of η (see Fig. 8a), and for *dp* = 5 mm. Measurements of the DC power at the output port of the rectifier were performed by varying the power delivered to the primary resonator (P_{AC}, see Fig. 9), corresponding results are given in Fig. 10a. Considering that the typical power consumption of modern pacemakers is in the range of [10 µW, 1 mW] [22], in the case of *dp* = 1.5 mm a value of P_{AC} of 60 mW is definitely enough to provide the energy needed. In fact, from Fig. 10a it can be seen that when P_{AC} is higher than 60 mW, the DC power provided by the proposed link to a load of 1 MΩ is higher than 1 mW. While in the case of *dp* = 5 mm, a value of P_{AC} of 80 mW is needed to provide a DC power of 1 mW.

Measurements were also performed by varying the value of the resistive load representative of the input impedance of the pacemaker. Corresponding results are given in Fig. 10b. The absolute maximum of the DC output power was obtained for 330 kΩ, which is a value different from the one adopted in circuit optimizations. This is probably due to the tolerance with respect to the nominal value of the lumped elements adopted in designing the rectifier (see Fig. 9b). However, it can be noticed that the DC output power is nearly constant for a load in the range of [0.33, 1] MΩ. In fact, in the case of *dp* = 1.5 mm it is equal to 1.42 mW for a 330 kΩ load and to 1.4 mW for a 1 MΩ load. While, in the case of *dp* = 5 mm it is equal to 1 mW for a 330 kΩ load and to 0.9 mW for a 1 MΩ.

C. SAR Analysis

The compliance of the proposed system with respect to human electromagnetic exposure limits was also investigated.

At the operating frequency of the proposed WPT link the IEEE and the ICNIRP (International Commission on Non-Ionizing Radiation Protection) guidelines provide basic restrictions for electromagnetic fields in terms of the Specific Absorption Rate (SAR) [23]-[24].

The SAR measures the rate at which energy is absorbed by the human body when exposed to a radio frequency (RF) electromagnetic field. It is defined as the power absorbed per mass unit of tissue [23]:

$$SAR\ (W/Kg) = \frac{d}{dt}\left(\frac{dW}{dm}\right) = \frac{d}{dt}\left(\frac{dW}{\rho dV}\right) \qquad (3)$$

where *dW* is the incremental energy absorbed by, or dissipated in, an incremental mass *dm* contained in a volume element *dV* of density ρ.

Current guidelines impose limits on the peak spatial-averaged SAR, which is the peak SAR averaged on a reference mass of tissue, typically 1-g or 10-g [23]-[24]. In more detail, the exposure limit considering a mass of 10-g is 2 W/kg for head and trunk areas and 4 W/kg for limbs.

In order to verify the compatibility of the proposed system with these limits, full-wave simulations were performed with CST Microwave Studio.

In more detail, we calculated at 403 MHz the 10-g average SAR distribution for a power delivered to the transmitter (P_{AC}) of 80 mW, which is the value guaranteeing a DC output power of about 1 mW. The configuration adopted in full-wave simulations is the one using three-tissue layers as illustrated in Fig. 2c. As for the relative positions assumed for the two resonators, both the case of aligned and misaligned resonators were considered. Results obtained in this way for *dp* = 5 mm are given in Figs. 11 (a)-(f).

Fig. 11a shows results corresponding to aligned resonators.

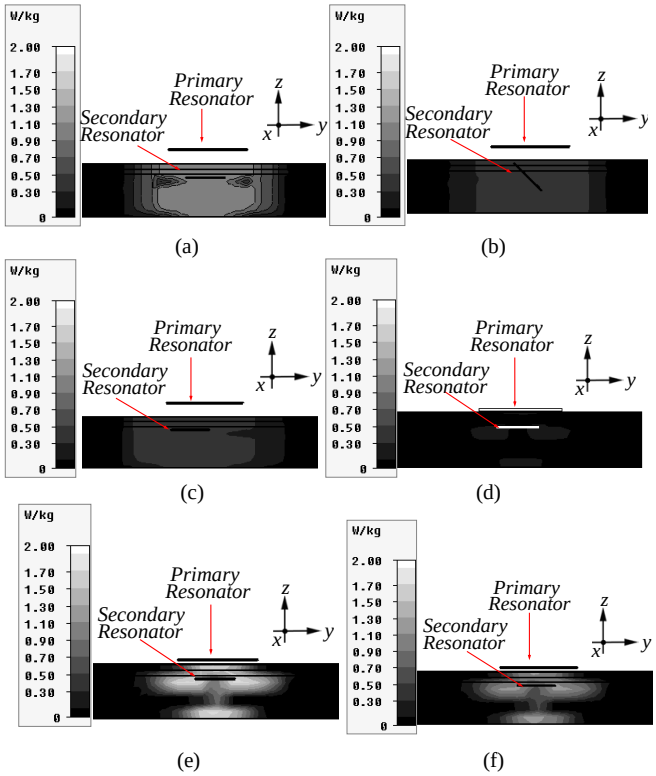

Fig. 11. Simulated 10-g average SAR distribution at 403 MHz. (a)-(c) Results obtained for dp = 5 mm and P_{AC} = 80 mW: (a) aligned resonators, (b) secondary resonator tilted of a 45° angle with respect to the xy plane (i.e., Case A of Fig. 8a), (c) a displacement $d_x = d_y = L_r/2$ of the two resonators with respect to the aligned position (i.e., Case B of Fig. 8a). (d)-(f) Results obtained for: (d) dp = 0 and P_{AC} = 80 mW, (e) dp = 1.5 mm and P_{AC} = 80 mW, (f) dp = 1.5 mm and P_{AC} = 60 mW. The density assumed for the three layers of human tissue was: 1109 kg/m³ for skin, 911 kg/m³ for fat and 1090 kg/m³ for muscle.

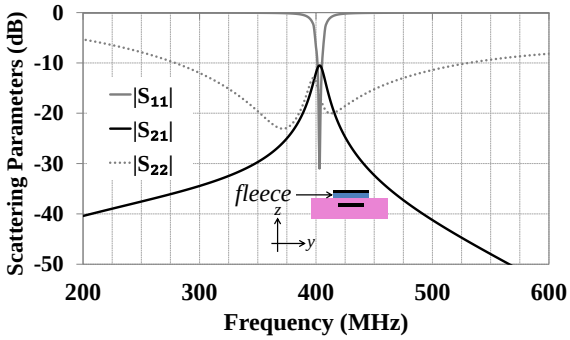

Fig. 12. Measured data of the scattering parameters obtained by placing the primary resonator on a 2 mm layer of fleece and thus directly on the skin (see the inset).

From full-wave simulations, for dp = 5 mm and P_{AC} = 80 mW the proposed inductive link complies with safety regulations. In fact, in this case the 10-g average SAR calculated by means of full-wave simulations is lower than 1.08 W/kg.

As for the case of misalignment, results obtained for a rotation of 45° of the secondary resonator around the x-axis (i.e., for the configuration named case A in Fig. 8a) and for a displacement $d_x = d_y = L_r/2$ (i.e., for the configuration named case B in Fig. 8a) are given in Figs. 11 (b)-(c), respectively. As expected, the values calculated for the 10-g average SAR are lower than the ones calculated for the case of aligned resonators.

The safety of the proposed system for different values of the distance of the primary resonator from the skin was also investigated. More specifically, we considered the case of dp = 0, which corresponds to the primary resonator placed on the skin, and the case of dp = 1.5 mm, which is the configuration corresponding to a maximum of η (see Fig. 8a). Figure 11d shows the 10-g average SAR distribution calculated for dp = 0. Consistently with the fact that for dp = 0 the power transfer efficiency of the proposed link is nearly zero, very low values were calculated.

Conversely, values very close to the 2 W/kg exposure limit imposed by safety regulations were obtained for dp = 1.5 mm and P_{AC} = 80 mW (see Fig. 11e). However, it should be noticed that for dp = 1.5 mm P_{AC} could be lowered to 60 mW. In fact, as observed in the previous section, this value is enough to guarantee a DC output power of 1 mW. Fig. 11f shows the SAR distribution calculated for P_{AC} = 60 mW and dp = 1.5 mm. Similarly to the case of dp = 5 mm, values definitely lower than 2 W/kg were obtained.

These results suggest that the proposed energy link complies with safety regulations when set to guarantee an output DC power lower than 1 mW. Some comments on these results are reported in the next section.

IV. Discussion on Results

With reference to the practical use of the proposed WPT system, and considering results reported in the previous section, it should be recognized that it might not be easy for the user to place the primary resonator as to ensure optimum alignment with the secondary resonator.

With regard to possible errors on dp (i.e., the distance from the skin of the primary resonator), it can be observed from Fig. 8a that, with respect to the value measured for a distance of 5 mm (i.e., -12.7 dB), the conversion efficiency assumes higher values for a distance greater than 0.5 mm, while it quickly goes to zero as dp becomes smaller. Furthermore, if we set P_{AC} to 80 mW (i.e., the value guaranteeing a DC output power of about 1 mW for dp = 5 mm), the induced SAR could be too high for distances in the range of [0.5, 5] mm.

This problem can be easily fixed by using an appropriate package guaranteeing that the primary resonator can be easily used at a distance larger than 0.5 mm from the skin. In particular, a solution could be to use of a foam layer (ε_r ~1) with a thickness in the range of [1, 5] mm to separate the primary resonator from the skin. The use of a foam with permittivity similar to air would not affect the performance of the proposed link. Alternatively, the primary resonator could be placed on a layer of textile fabric that could be directly placed on the skin. In this regard, referring to the inset of Fig. 12, we experimentally investigated the performance of the proposed WPT link when the primary resonator is placed on a 2 mm layer of fleece (ε_r =1.12). Scattering parameters obtained in this way are given in Fig. 12. It can be noticed that the presence of the fleece layer has a positive effect on the performance of the link. In more detail, a maximum of -

10.5 dB was obtained for the amplitude of the transmission coefficient in presence of the 2 mm layer of fleece, while the value measured at the same distance without fleece was -11.3 dB.

As for errors concerning a displacement along the *x*- and the *y*- axis, they could be minimized by placing the primary resonator on a jacket as to have a reference.

However, despite various measures can be taken, user errors in positioning the primary resonator are possible so that the use of a control unit should be considered, similar to the one present in current pacemaker. In more detail, the control unit should monitor the level of the power delivered to the pacemaker and it should emit an alert signal when this power is below or above a threshold value.

Another point that should be taken into account for the practical adoption of the proposed system, is related to the possibility of having a shift of the resonance frequency of the secondary resonator after implantation.

This problem can be easily fixed by using a varactor for the lumped capacitor illustrated in Fig. 2a. In this way, by varying the capacitance of the varactor, the resonance frequency of the primary resonator could be tuned as to lock the resonance frequency of the secondary resonator.

The same control unit used for verifying errors on the relative position of the two resonators could be used for verifying that the two resonators are tuned. However, it is expected that the resonance frequency of the secondary resonator does not change significantly during the various uses of the device, so this check should be performed only during the first uses.

V. Conclusion

A wireless power link for implantable medical devices has been presented. The proposed system operates in the MedRadio service core band and consists of two inductively coupled resonators. Experimental tests demonstrating its suitability to be used for powering pacemakers are reported and discussed. It is shown that the proposed link is able to satisfy the typical power consumption of modern pacemakers in compliance with safety regulations. In fact, from experimental data combined with full-wave simulations it is shown that the proposed system provides up to 1 mW with an induced 10-g average SAR lower than 1.08 W/kg.

References

[1] Z. N. Chen, G. C. Liu, and T. S. P. See, "Transmission of RF signals between MICS loop antennas in free space and implanted in the human head," *IEEE Trans. Antennas Propag.*, vol. 57, no. 6, pp. 1850–1853, Jun. 2009.

[2] J. Kim and Y. Rahmat-Samii, "Implanted antennas inside a human body: Simulations, designs, and characterizations," *IEEE Trans. Microw. Theory Techn.*, vol. 52, no. 8, pp. 1934–1943, Aug. 2004.

[3] P. Soontornpipit, C. M. Furse, and Y. C. Chung, "Design of implantable microstrip antennas for communication with medical implants," *IEEE Trans. Microw. Theory Techn.*, vol. 52, no. 8, pp.1944–1951, Aug. 2004.

[4] M. Asili, R. Green, S. Seran, and E. Topsakal, "A Small Implantable Antenna for MedRadio and ISM Bands," *IEE Antenn. and Wireless Propag. Lett.*, vol. 11, pp. 1683-1685, Jan. 2012.

[5] *Medical Device Radiocommunications Service (MedRadio)*, Federal Communications Commission (FCC), 2009.

[6] K. Goto, T. Nakagawa, and S. Kawata, "An Implantable Power Supply with an Optically Rechargeable Lithium Battery," *IEEE Trans. Biomed. Eng.*, vol. 48, no. 7, pp. 830-833, July 2001.

[7] P. Li and R. Bashirullah, "A Wireless Power Interface for Rechargeable Battery Operated Medical Implants," *IEEE Trans. Circuits Systems*, vol. 54, no. 10, pp. 912-916, Oct. 2007.

[8] X. Qi, G. Zhaolong, W. Hao, H. Jiping M. Zhi-Hong, and S. Mingui, "Batteries Not Included: A Mat-Based Wireless Power Transfer System for Implantable Medical Devices As a Moving Target," *IEEE Microw. Magaz.*, vol. 14, no. 2, pp. 63-72, Mar.-Apr. 2013.

[9] K. Jung, Y. H. Kim, E. Jung Choi, H. Jun Kim, and Y. J. Kim, "Wireless Power Transmission for Implantable Devices Using Inductive Component of Closed-Magnetic Circuit Structure," in *Proc. IEEE Intern. Conf. Multis. Fusion Integr. Intell. Syst.*, 2008, pp. 272-277.

[10] U. M. Jow and M. Ghovanloo, "Modeling and optimization of printed spiral coils in air, saline, and muscle tissue environments," *IEEE Trans. Biomed. Circuits Systems*, vol. 45, no. 1, pp. 21-22, Aug. 2009.

[11] R. F. Xue, K. W. Cheng, and M. Je, "High-Efficiency Wireless Power Transfer for Biomedical Implants by Optimal Resonant Load Transformation," *IEEE Trans. Circuits Systems*, vol. 60, no. 4, pp. 867-874, Aug. 2013.

[12] A. Khripkov, W. Hong, and K. Pavlov, "Integrated Resonant Structure for Simultaneous Wireless Power Transfer and Data Telemetry," *IEEE Antennas Wireless Propag. Lett.*, vol. 11, pp. 1659-1662, Jan. 2012.

[13] A. S. Y. Poon, S. O'Driscoll, and T. H. Meng, "Optimal Frequency for Wireless Power Transmission Into Dispersive Tissue," *IEEE Trans. Antennas Propag.*, vol. 58, no. 5, pp. 1739-1750, Mar. 2010.

[14] A. J. Yeh, J. S. Ho, Y. Tanabe, E. Neofytou, R. E. Beygui, and A.S.Y. Poon, "Wirelessly powering miniature implants for optogenetic stimulation," *Appl. Phys. Lett.*, vol. 103, no. 16, Oct. 2013.

[15] D. Pivonka, A. Yakovlev, A. S. Y. Poon, and T. Meng, "A mm-Sized Wirelessly Powered and Remotely Controlled Locomotive Implant," *IEEE Trans. Biomed. Circuits Systems*, vol. 6, no. 6, pp. 21-22, Jan. 2013.

[16] G. Monti, L. Tarricone, and C. Trane, "Experimental Characterization of a 434 MHz Wireless Energy Link For medical Applications," *Progr. Electromag. Research C*, vol. 30, pp. 53-64, May 2012.

[17] P. Gay-Balmaz and O. J. F. Martin, "Electromagnetic resonances in individual and coupled split-ring resonators," *Journ. Appl. Phys.*, vol. 92, no. 5, pp. 2929-2936, Sept. 2002.

[18] G. Haobijam and R. P. Palathinkal, *Design and Analysis of Spiral Inductors*. Spinger India, 2014.

[19] P. A. Hasgall, F. Di Gennaro, C. Baumgartner, E. Neufeld, M. C. Gosselin, D. Payne, A. Klingenböck, and N. Kuster, "IT'IS Database for thermal and electromagnetic parameters of biological tissues," version 2.5, Aug. 2014.

[20] F. J. Huang, C. M. Lee, C. L. Chang, L. K. Chen, T. C. Yo, and C. H. Luo, "Rectenna Application of Miniaturized Implantable Antenna Design for Triple-Band Biotelemetry Communication," *IEEE Trans. Antennas Propagat.*, vol. 59, no. 7, pp. 2646-2653, May 2011.

[21] C. K. Wu, T. F. Chien, C. M. Cheng, C. L. Yang, and C. H. Luo, "Development of Wideband Miniaturized Antennas by Fringe Field Capacitance Effects for Implantable MedRadio Band Biotelemetry," *Journ. Med. Biolog. Eng.*, Jan. 2013.

[22] J. H. Oh, T. H. Kim, J. H. Yoo, J. K. Pack, Y. M. Yoon, M. Y. Choi, and S. Y. Lee, "Human Exposure Assessment for Wireless Power Transmission System," *PIERS Proceedings*, Xi'an, China, Mar. 22-26, 2010.

[23] IEEE Standard for Safety with Respect to Human Exposure to Radio Frequency Electromagnetic Fields, 3 kHz to 300 GHz, IEEE Standard C95.1-1991, 1999.

[24] ICNIRP, "Guidelines for limiting exposure to time-varying electric, magnetic, and electromagnetic fields (up to 300 GHz)," *Health Phys.*, vol. 74, no. 4, pp. 494–522, Oct. 1998.

Giuseppina Monti received the Laurea degree in telecommunication engineering (with honors) from the University of Bologna, Bologna, Italy, in 2003, and the Ph.D.degree in information engineering from the University of Salento, Lecce, Italy, in 2007.

She is currently with the Department of Innovation Engineering, University of Salento, Lecce, Italy, as a Temporary Researcher and Lecturer in CAD of microwave circuits and antennas. Her current research interest includes the analysis and applications of artificial media, the design and realization of microwave components, MEMS-based reconfigurable antennas and devices, rectennas, and systems and devices for wireless power transmission applications. She has coauthored a book chapter and approximately 100 papers in international conferences and journals.

Paola Arcuti received the M.S. degree in telecommunications engineering (cum laude) and Ph.D. degree in information engineering from the University of Salento, Lecce, Italy, in 2010 and 2014, respectively. Her research activity includes the design of wireless power transfer systems for applications in medical field, the development of novel biotelemetry systems for monitoring human vital signs and the study of energy harvesting systems for sensor powering

Luciano Tarricone received the Laurea degree in electronic engineering (*cum laude*) and Ph.D. degree from Rome University "La Sapienza," Rome, Italy, in 1989 and 1994, respectively.

From 1990 to 1992, he was a Researcher with the IBM Rome Scientific Centers. From 1992 to 1994, he was with the IBM European Center for Scientific and Engineering Computing, Rome, Italy. Between 1994 and 1998, he was a Researcher with the University of Perugia, Perugia, Italy, and, between 1998 and 2001, he was a "Professore Incaricato" of electromagnetic (EM) fields and EM compatibility. Since November 2001, he has been a Faculty Member with the Department of Innovation Engineering, University of Salento, Lecce, Italy, where he is Full Professor of EM fields and coordinates a research group of about 15 people. He has authored and coauthored approximately 300 scientific papers. His main contributions are in the modeling of microscopic interactions of EM fields and biosystems, and in numerical methods for efficient CAD of microwave circuits and antennas. He is currently involved in bioelectromagnetics, electromagnetic energy harvesting and wireless power transmission, novel CAD tools and procedures for microwave circuits, RFID, and EM high-performance computing.